Paper 4

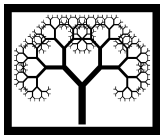

Proceedings of the Eleventh International Conference
on Computational Structures Technology,
B.H.V. Topping, (Editor),
Civil-Comp Press, Stirlingshire, Scotland

Finite Element Analysis of Failure Modes for Cellular Steel Beams

B. Dervinis and A.K. Kvedaras
Vilnius Gediminas Technical University
Lithuania

Abstract

This paper considers the numerical non-linear analysis of the behaviour of the cellular steel beams taking into account the geometrical and physical nonlinearities. Nowadays, the analysis of the cellular steel beams is well investigated. Therefore, it is not difficult to obtain and verify the load bearing capacity values for a member with known dimensions. However, it might be difficult for a known value of applied load to obtain a section with the rational dimensions. The purpose of this paper is to illustrate graphically the different modes of failure for the cellular steel beams investigated, comparing their behaviour under different values of ultimate load for different sections with different modes of failure and stress distribution. In this paper a method is developed for selecting a cellular steel beam section with the rational dimensions and parameters for a known load using finite element analysis and existing software. Therefore, the concept of selection of rational sectional parameters for the steel beams with the multiple openings, based on the data of the numerical analysis carried out, is presented as well. Hence the following conclusions are drawn: 1) It is important to select the rational section dimensions because that would enable the best use of the steel and provides economic solutions; 2) The concept of simple selection of rational section dimensions significantly improves the steelwork design process.

Keywords: cellular steel beam, rational section‘s dimensions, non-linear analysis, applied software, finite element analysis, failure modes.

1 Introduction

According to the point of view of the material mechanics, the beam cross-section is more efficient, if more material is concentrated in the flanges and less in the web [1]. The cellular beam shown in Figure 1 has the multiple web openings and, therefore, its web is lighter than of the ordinary steel beam.

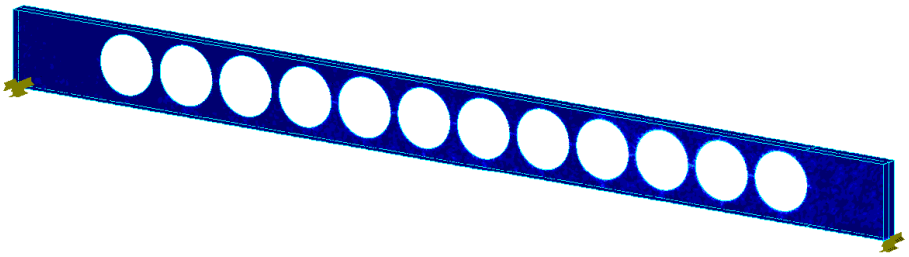

Figure 1. Cellular steel beam

The cellular steel beams are widely used in commercial, industrial, residential and other buildings. Due to the web openings such beams are very attractive for buildings with a big amount of different communications, because of possibility passing them strightly through the web of beams. The height of the room may be saved, what is very important in high buildings. The beautiful view of ceiling with the cellular beams as an advantage could be mentioned as well. In Figure 2 the parking in Lausanne, Switzerland is shown.

Figure 2. Parking in Lausanne, Switzerland (photo by T. Serafinavičius)

The beams used nowadays are not only made of rolled sections, but also built up using steel plates [2]. Using such beams allows us to dispose all cross-sectional dimensions and find the rational ones. According to the experimental data, 8 failure modes of beams with web openings are known [3], [4] and [5]. It is a flexural mechanism, lateral-torsional buckling, distortional buckling, web post buckling due to shear force, web post buckling due to compression force, Vierendeel or shear mechanism, rupture of welded joints, ultimate deflecting.

2 Scope and aim of the investigation

The coveted aim of this paper is reviewing and illustrating graphically the different modes of failure for cellular beams. For this purpose the finite element method (FEM) was invoked. Six different beams are analysed under different loading and different supporting conditions. The modes of failure depend on cross-sectional dimensions, length of the beam, restraints and load type. It is determined influence

of cellular steel beam dimensions beams on the modes of their failure. Other aim of this paper is presenting an idea for developing the algorithm of selection the rational cross-sectional dimensions for cellular steel beams using the finite element method.

3 Finite element modelling

For FEM modelling the finite element software COSMOSM was selected. SHELL3T is used as a type of finite elements. SHELL3T is 3-node thick shell element with membrane and bending capabilities for nonlinear analysis of 3D structural models. The element accounts for shear deformation effects. Six degrees of freedom (three translations and three rotations) are considered per node. In order to simulate the structural behaviour of cellular steel beams, a finite element model is established with material non-linearity. A bi-linear stress-strain curve, as shown in Figure 3, is adapted in the material modelling of steel grade S355.

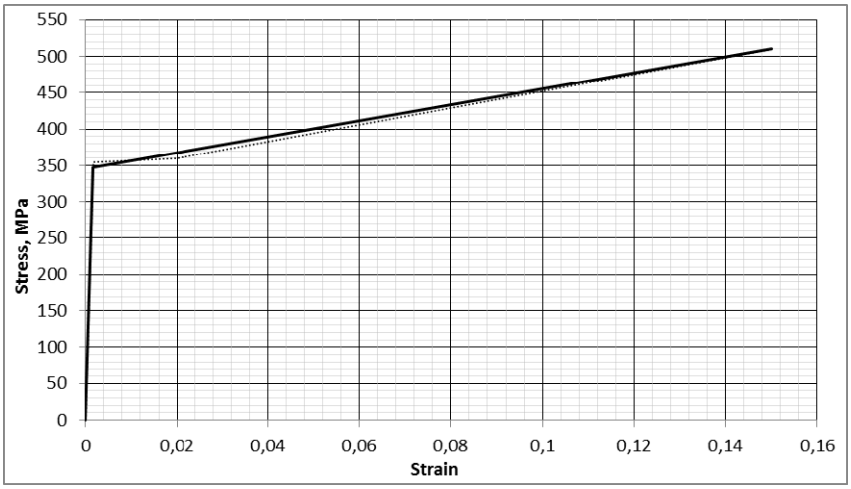

Figure 3. Stress-strain curve of steel of modelled beams

Moreover, the geometric non-linearity is incorporated into the finite element model, so the large deformation in the model may be accurately predicted, allowing load redistribution in the web across the opening after initial yielding.

The finite element mesh density is presented in Figure 4. A circular opening is formed in the web with refined mesh configuration.

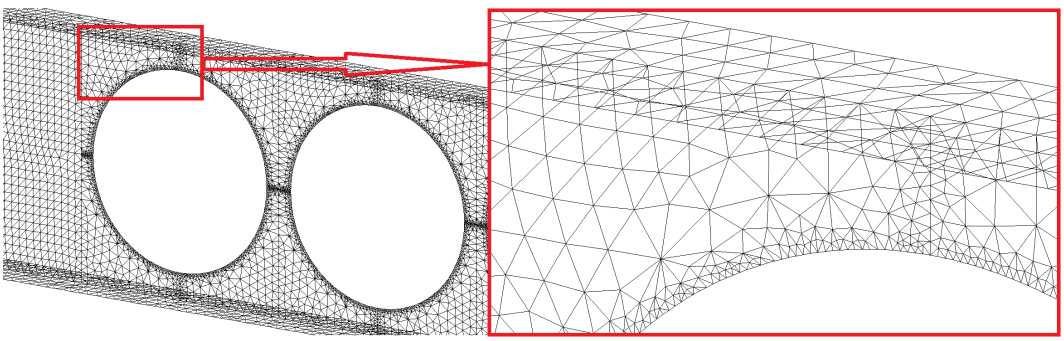
Figure 4. Distribution of the finite elements in the model of the cellular steel beam

After sensitivity studies on the density of the finite element mesh, the finite element size was chosen about 3…4 cm. Moreover, the density of finite element mesh is increased around the each opening edge and it is 360 finite elements along it. Finite element models for cellular beams consisted from 34624 to 47048 finite elements. The calculations were made with iterations as the analysis was geometrically and physically non-linear. The Newton-Raphson iterative technique for arc-length control was selected in calculations. The maximum load parameter was chosen as 1000. The calculations stopped when the maximum stress values were reached, when the node's displacement exceeded the ultimate value or it started to increase very rapidly without sufficient load increasing. At the end of calculations (at the last load step) the load parameter was adopted as a multiplier to get ultimate load. Since the geometrically and physically nonlinear analysis was performed, the values of stresses, nodal displacements and buckling load may be received from the results of a single calculation.

4 Failure modes of cellular steel beams

In this chapter the six failure modes from existing eight ones of cellular steel beams are presented. Due to reason, that ultimate deflecting and rupture of welded joints failure modes are not attractive from point of view of graphical illustration, they are not represented in this paper. It is observed that when beam's length is big (over six, seven meters) one of the main failure modes is the ultimate deflecting, of course if the beam is well designed. The aim of this paper is not to design well the cellular steel beams, but to show deformed shape of the beams and stress distribution in their cross-section. The beam parameters, used in calculations are: b_f – flange width, t_f – flange thickness, h_w – web depth, t_w – web thickness, d – diameter of opening, a – distance between openings, L – beam length, p – ultimate uniform load, F – ultimate concentrated force, f – ultimate deflection, M – weight of the beam, R – rationality factor (R=(Total load)/M [kN/kg]). Some of the beam geometrical parameters are presented in Figure 5.

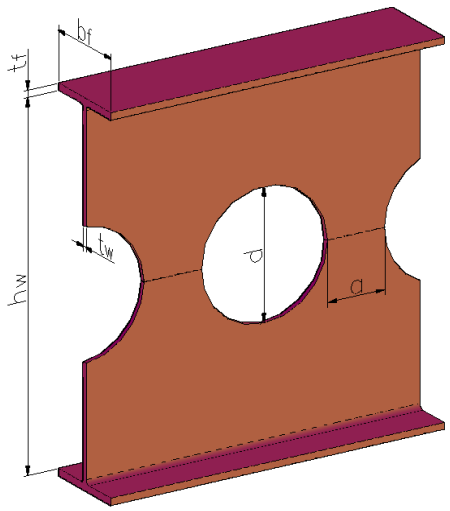

Figure 5. Beam's geometrical parameters

For the better view below the pictures of the deformed shape and stresses in the beam cross-section are presented for a half beam.

4.1 Failure mode – flexural mechanism

Flexural mechanism can occur in the beams then the steel in the T-sections below and above the openings yields under action of bending moment until the plastic hinges are formed. The yielding in the T-sections is very similar to the yielding in solid web beams. Such form of failure can occur for not very long (up to six, seven meters) beams with thick web, small flanges and not very big, comparing with beam's depth, openings. In other cases another failure mode can occur.

The beam analysed at the flexural mechanism failure mode is presented in Figure 6. This beam is simply supported and upper flange along all length is restrained out of plain. Beam is loaded with uniformly distributed load. The beam parameters are: b_f=120 mm, t_f=16 mm, h_w=800 mm, t_w=12 mm, d=350 mm, a=160 mm, L=7000 mm, p=180.0 kN/m, f=35 mm, M=629.8 kg, R=2.000 kN/kg.

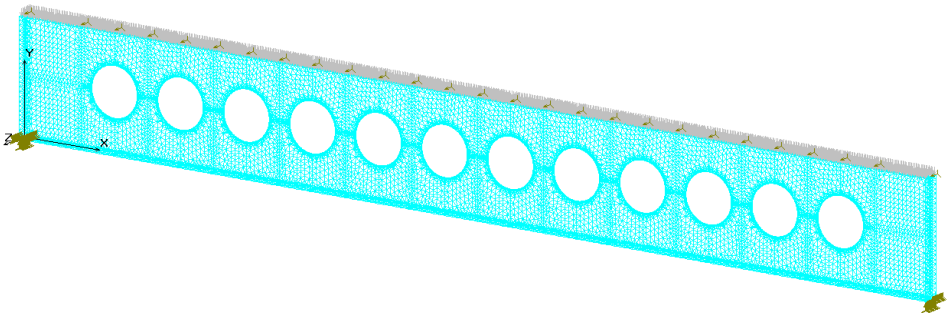

Figure 6. The supporting and loading model of the beam analysed at the flexural mechanism failure mode

Deformed shape of the beam at the flexural mechanism failure mode is presented in Figure 7. As very common case, beam just deflected under the action of uniform load. It can be noted, that beam's deflection also reached the ultimate value, as well as the stresses presented in below following figures.

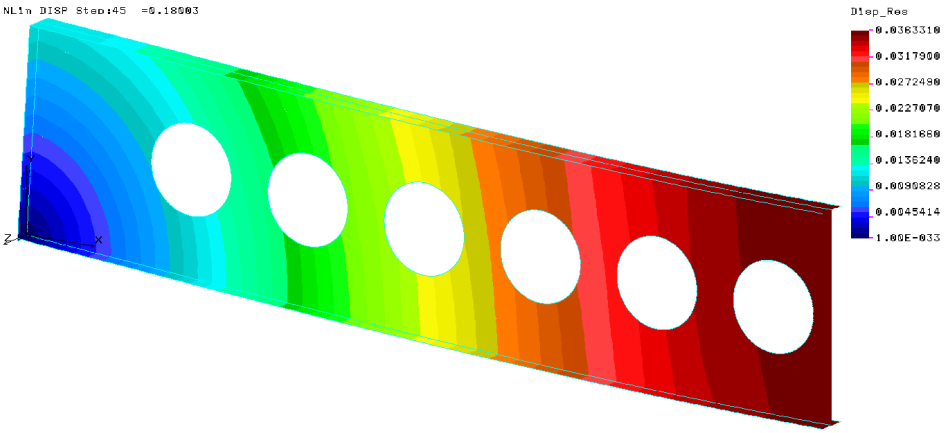

Figure 7. Deformed shape of the beam at the flexural mechanism failure mode

From the Figure 8 it is seen that the stresses in some beam's cross-sections reached the values of yielding stresses.

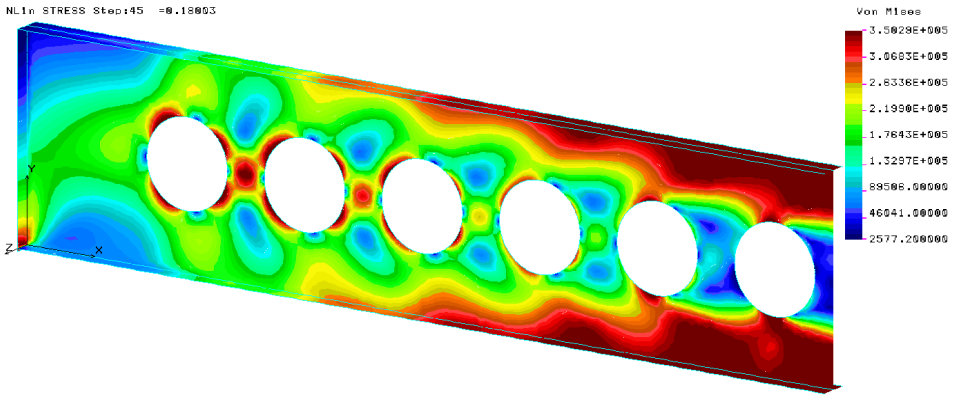

Figure 8. Distribution of the Von Mises stresses along the beam at the flexural mechanism failure mode

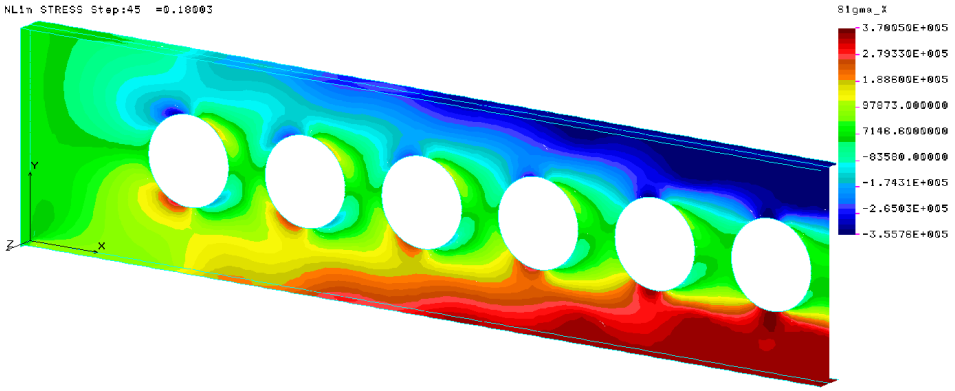

Figure 9. Distribution of stresses σ_x along the beam at the flexural mechanism failure mode

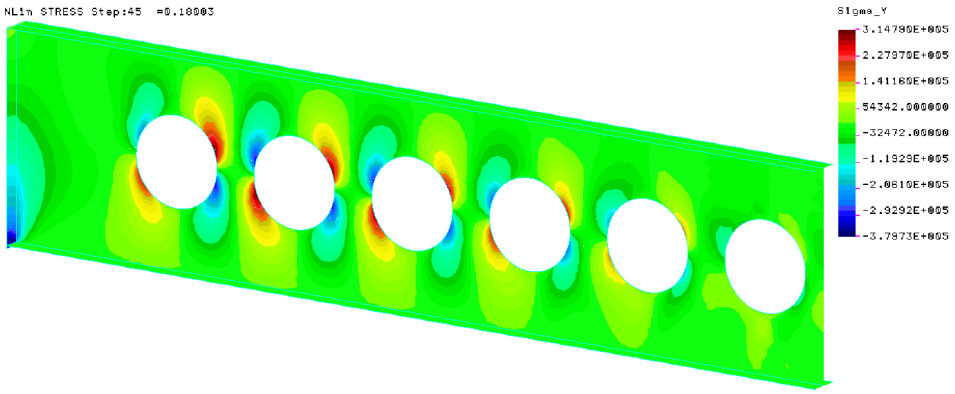

Figure 10. Distribution of stresses σ_y along the beam at the flexural mechanism failure mode

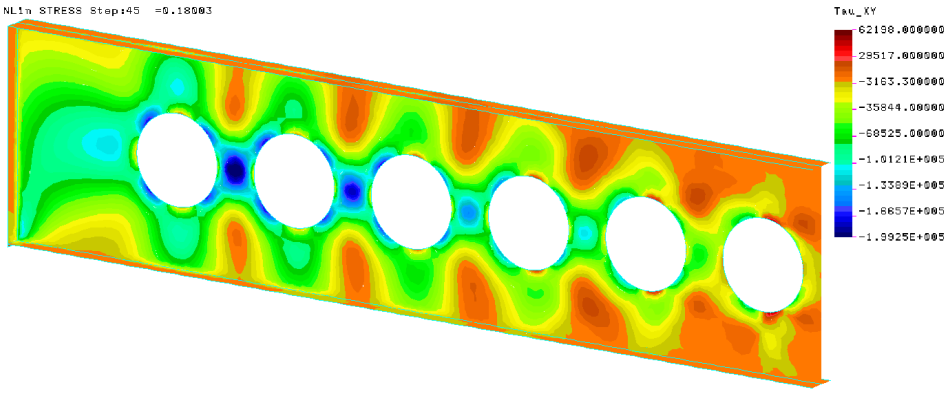

Figure 11. Distribution of stresses τ_{xy} along the beam at the flexural mechanism failure mode

The main component of the Von Mises stresses is σ_x as it could be seen in Figure 9. Distribution of other stress components is presented in Figures 10 and 11. The beam's material is fully used up when it fails due to flexural mechanism.

4.2 Failure mode – lateral-torsional buckling

As in the usual beams the lateral-torsional buckling is characterised by out of plain deformations when web is straight and without any distortion. Usually lateral-torsional buckling occurs in long beams where dimensions between out of plain restraints are big. D. Kerdal and D. A. Nethercot [6] investigated this mode of failure. They found, that openings in the web have negligible effect on lateral-torsional buckling. Moreover, they proposed to calculate castellated steel beams for the lateral-torsional buckling as usual beams with geometrical characteristics of the beam with web openings. The same assumptions may be adapted to cellular beams.

The beam analysed at the lateral-torsional buckling failure mode is presented in Figure 12. This beam is simply supported and upper flange has no out of plain restraints. Beam is loaded with concentrated forces. The beams' parameters are: b_f=160 mm, t_f=16 mm, h_w=1000 mm, t_w=6 mm, d=700 mm, a=200 mm, L=12000 mm, F=25.5 kN, f=48 mm, M=830.0 kg, R=0.0615 kN/kg.

Deformed shape of the beam at the lateral-torsional buckling mode is presented in Figure 13. From the picture we can see, that the horizontal deflection is bigger than the vertical one and it reached the ultimate value.

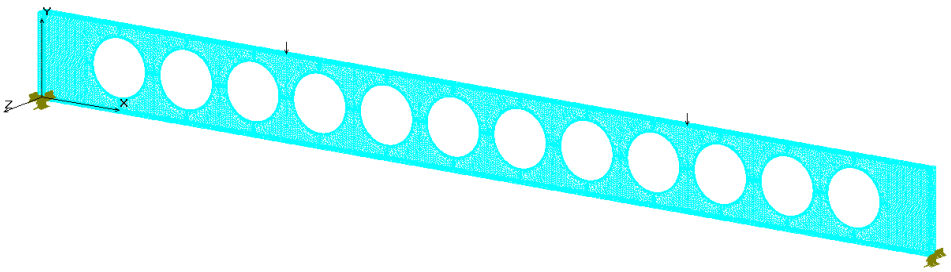

Figure 12. The supporting and loading model of the beam analysed at the lateral-torsional buckling failure mode

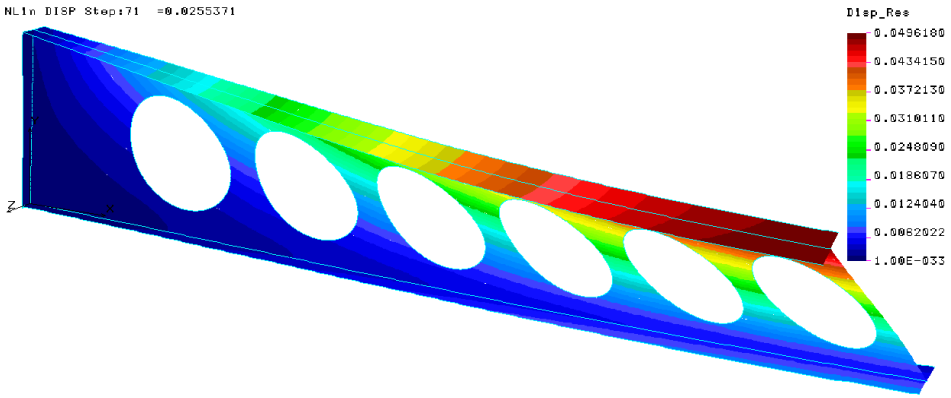

Figure 13. Deformed shape of the beam at the lateral-torsional buckling failure mode

From the Figures 14–17 it is seen that the stresses in the beam's cross-sections did not reach the values of yield stresses. The compression stresses σ_x causes the failure of the beam. Upper flange of the beam just buckled out of plain. By analysing the stress distribution after buckling it is seen, that the tension stresses σ_x in the bottom flange are distributed uniformly and the stresses σ_x in the top flange are of different signs. Moreover, the compression stresses in the top flange are bigger than tension stresses.

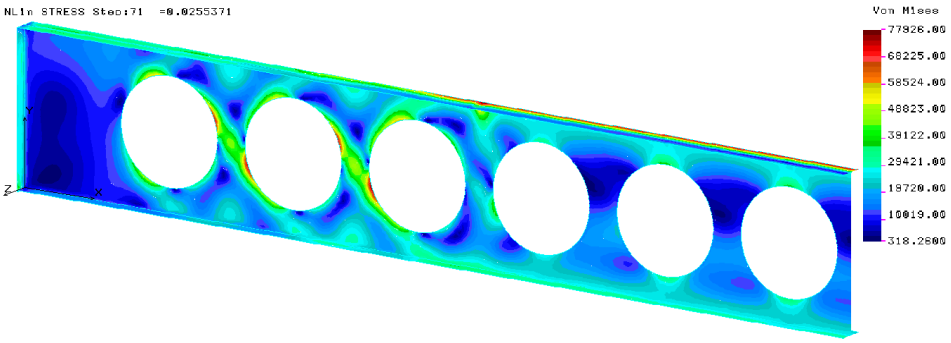

Figure 14. Distribution of the Von Mises stresses along the beam at the lateral-torsional buckling failure mode

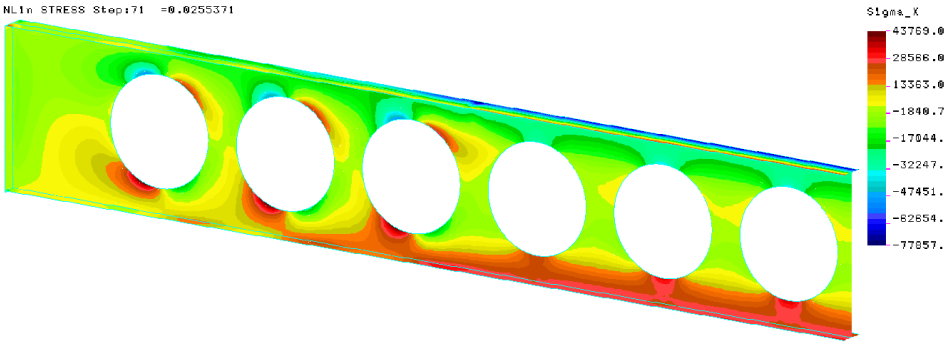

Figure 15. Distribution of the stresses σ_x along the beam at the lateral-torsional buckling failure mode

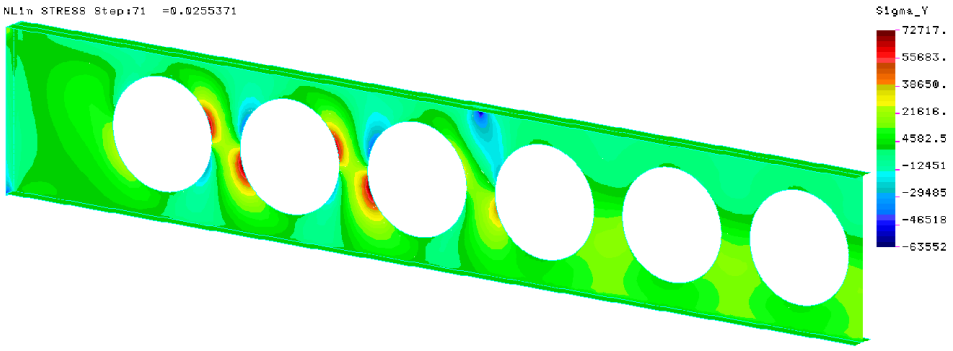

Figure 16. Distribution of the stresses σ_y along the beam at the lateral-torsional buckling failure mode

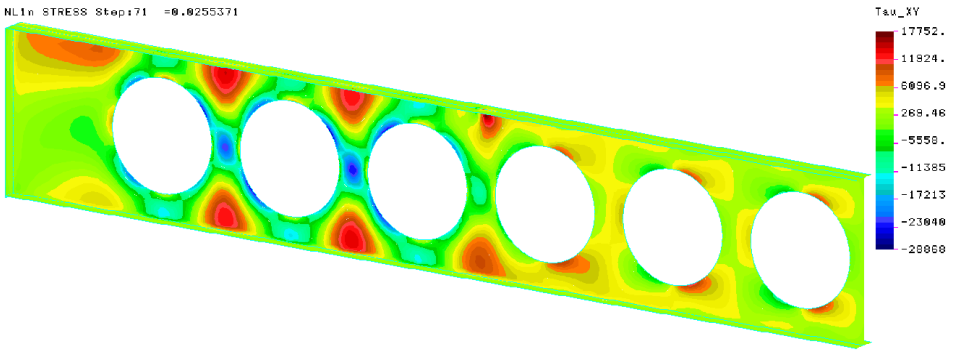

Figure 17. Distribution of the stresses τ_{xy} along the beam at the lateral-torsional buckling failure mode

4.3 Failure mode – distortional buckling

Distortional buckling is mode of failure when at the same time a cross-section of the beam becomes distorted and moves out of plain. Due to this reason, flanges of the beam twist with different angles, what reduces the buckling resistance of the beam. This mode of failure could occur in the beams with an intermediate length and with a slender web. Distortional buckling is as a result of two failure modes (local and lateral buckling) compounded in the one.

The beam analysed at the distortional buckling failure mode is presented in Figure 18.

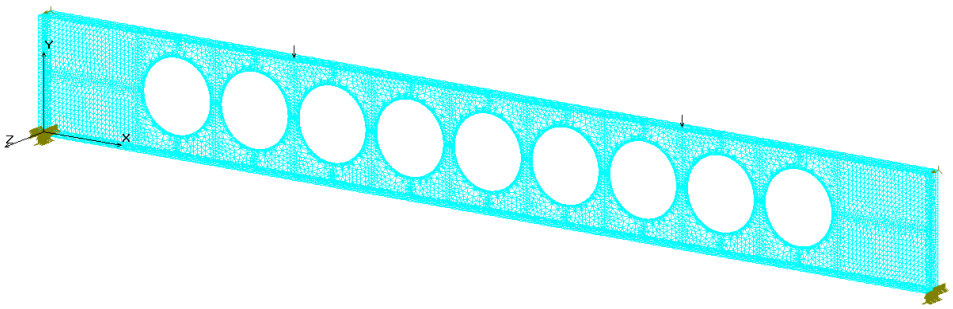

Figure 18. The supporting and loading model of the beam analysed at the distortional buckling failure mode

This beam is simply supported, and its upper flange is restrained out of plain at force application places. Beam is loaded with concentrated forces. The beam parameters are: b_f=160 mm, t_f=16 mm, h_w=1000 mm, t_w=6 mm, d=700 mm, a=150 mm, L=9000 mm, F=100.6 kN, f=40 mm, M=640.6 kg, R=0.314 kN/kg.

Deformed shape of the beam at the distortional buckling failure mode is presented in Figure 19. From this picture it is seen that the value of the horizontal deflection is bigger than the value of the vertical one, and its value almost reached the ultimate value.

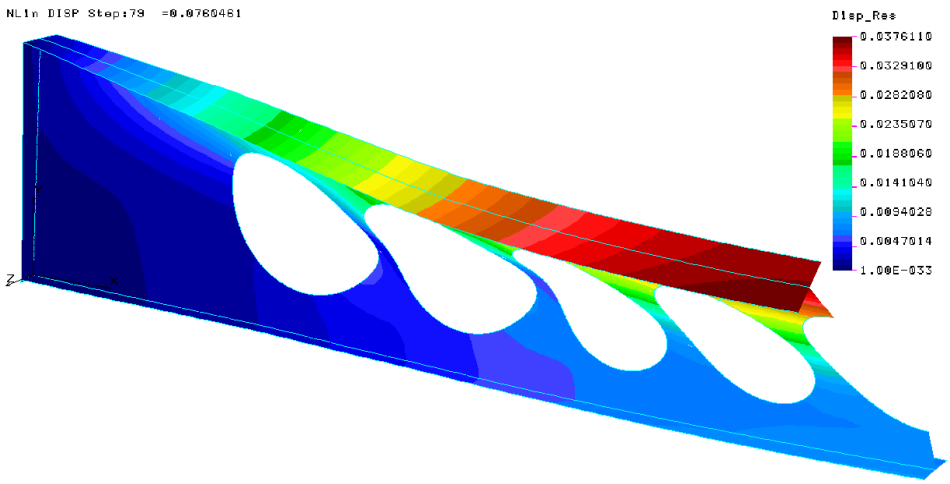

Figure 19. Deformed shape of the beam at the distortional buckling failure mode

From the Figures 20–23 it is seen that the values of stresses in the beam's cross-section around the end openings almost reached the value of the yield stresses. These stresses are not dangerous because they have a local character. This failure mode is a combination of two failure modes: a lateral-torsional buckling and web post buckling due to shear force.

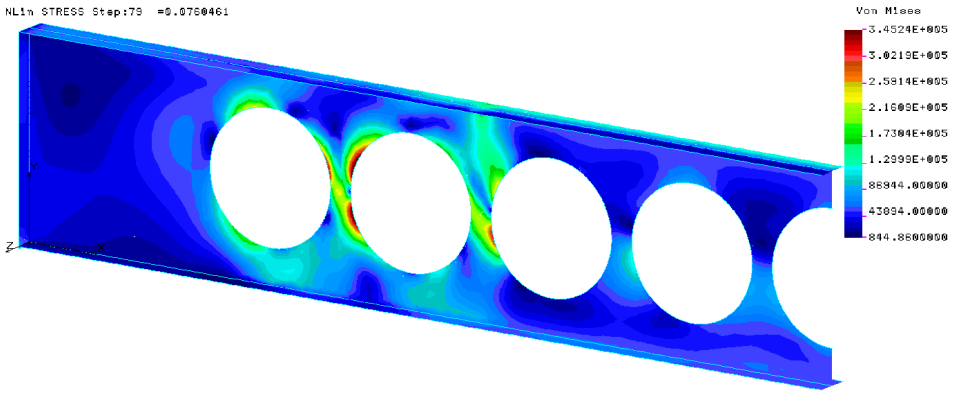

Figure 20. Distribution of the Von Mises stresses along the beam at the distortional buckling failure mode

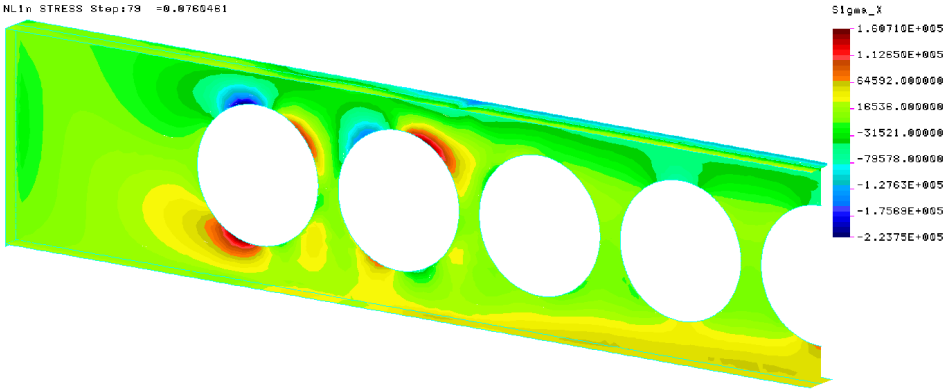

Figure 21. Distribution of the stresses σ_x along the beam at the distortional buckling failure mode

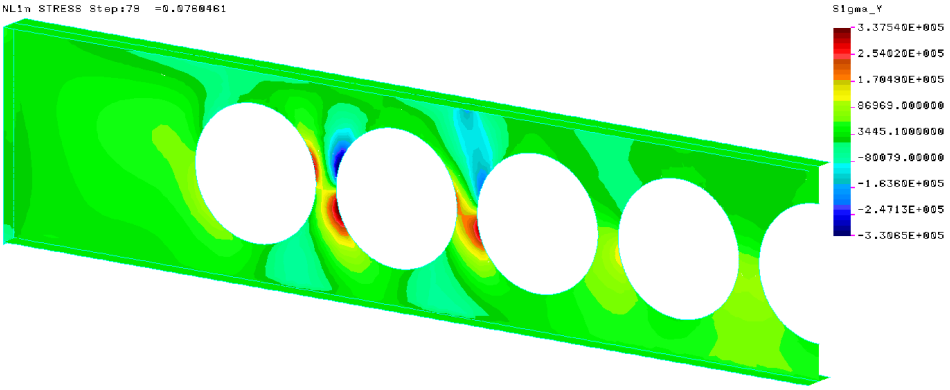

Figure 22. Distribution of the stresses σ_y along the beam at the distortional buckling failure mode

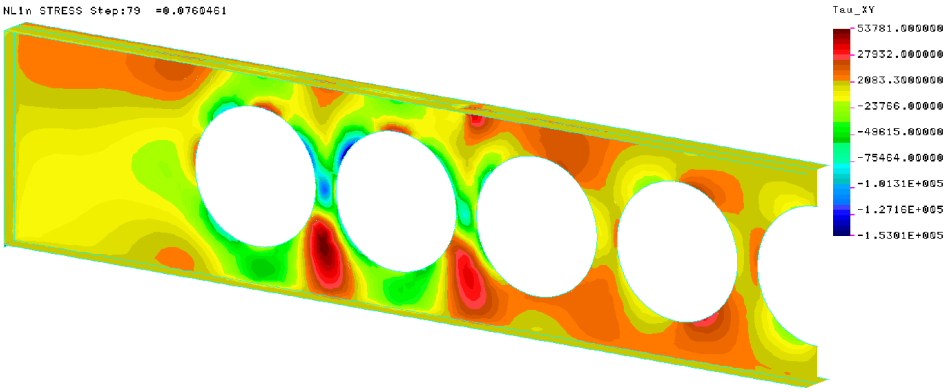

Figure 23. Distribution of the stresses τ_{xy} along the beam at the distortional buckling failure mode

4.4 Failure mode – web post buckling due to shear force

The web post under action of the horizontal share force becomes distorted and the form of distortion is like a propeller. The one inclined edge of the web post is under compression and the opposite one – under tension. Such stress distribution causes a

twist of the web post, or saying in other words the web post buckles under the share force.

The beam analysed at the web post buckling due to shear force failure mode is presented in Figure 24. This beam is simply supported and its upper flange along the all length is restrained out of plain. This beam is loaded with the uniformly distributed load. The beam parameters are: b_f=120 mm, t_f=16 mm, h_w=800 mm, t_w=8 mm, d=600 mm, a=150 mm, L=9000 mm, p=45.0 kN/m, f=40 mm, M=545.9 kg, R=0.742 kN/kg.

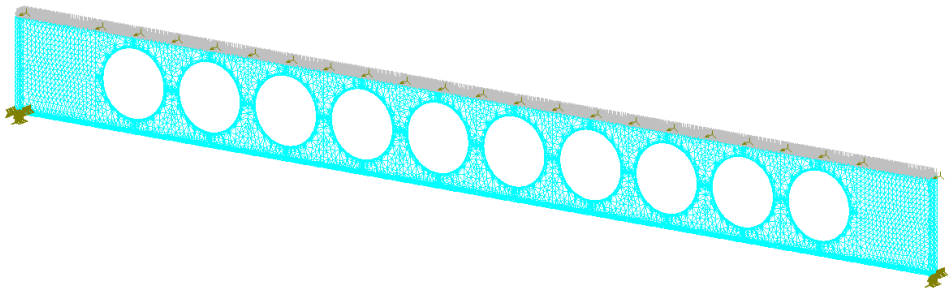

Figure 24. The supporting and loading model of the beam analysed at the web post buckling due to shear force failure mode

Deformed shape of the beam at the web post buckling due to shear force failure mode is presented in Figure 25. From this picture it is seen, that the value of the horizontal deflection is bigger than the value of the vertical one, and it reached the ultimate value.

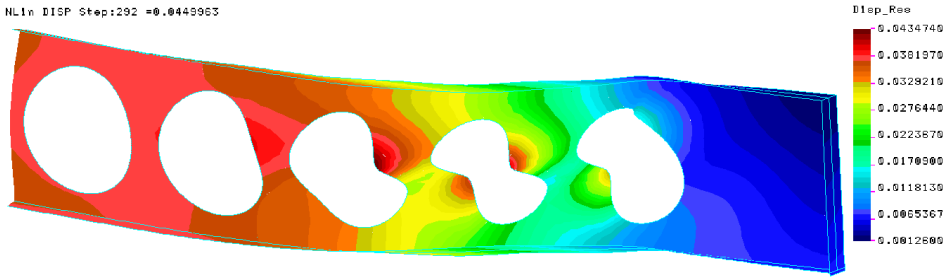

Figure 25. Deformed shape of the beam at the web post buckling due to shear force failure mode

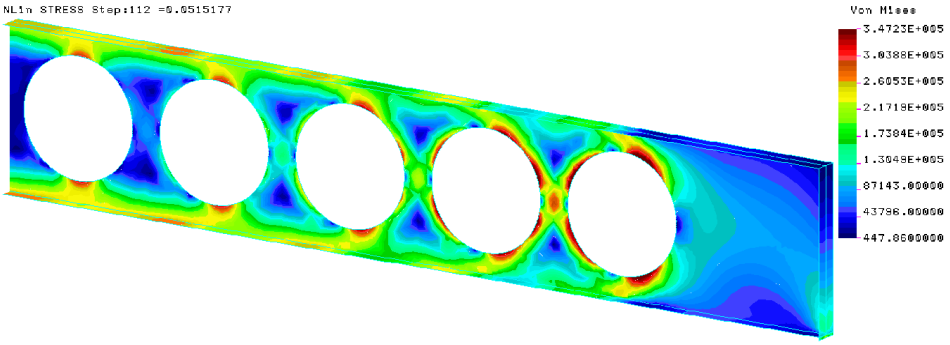

Figure 26. Distribution of the Von Mises stresses along the beam at the web post buckling due to shear force failure mode

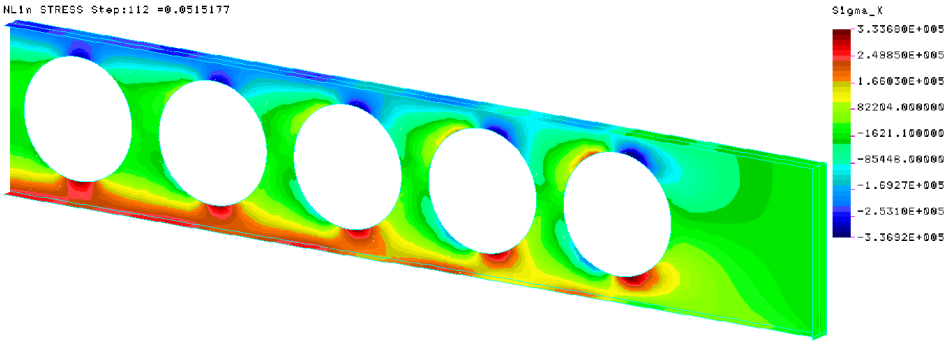

Figure 27. Distribution of the stresses σ_x along the beam at the web post buckling due to shear force failure mode

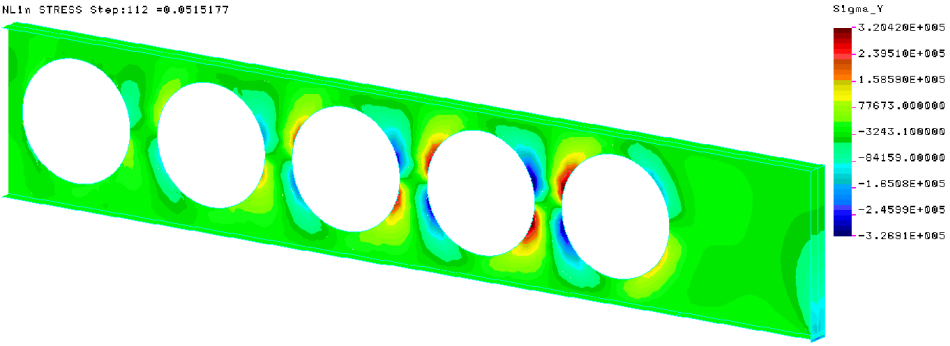

Figure 28. Distribution of the stresses σ_y along the beam at the web post buckling due to shear force failure mode

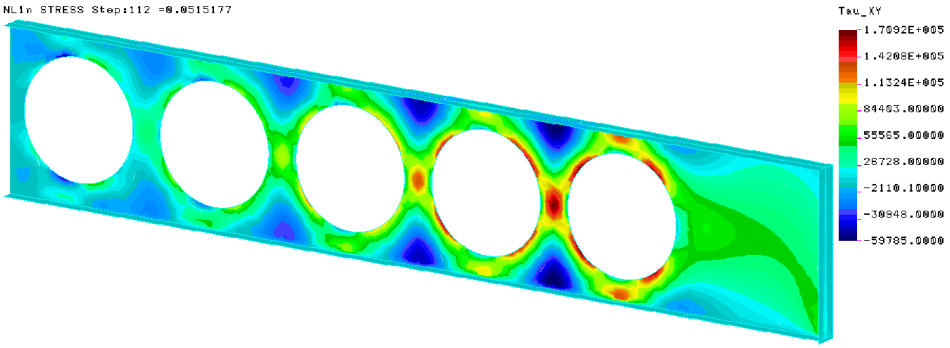

Figure 29. Distribution of the stresses τ_{xy} along the beam at the web post buckling due to shear force failure mode

From the Figures 26–29 it is seen that the values of the stresses in the beam's cross-section around the end openings and in the web post between those openings are extremely big. It can be assumed that the buckling of the web post is caused by all stress components, especially σ_y and τ_{xy}.

4.5 Failure mode – web post buckling due to compression force

This mode of failure can be caused by applying concentrate the force or the reaction above the web post. Web post buckles without any twisting unlike in the case with

web post buckling due to share force. For securing the load carrying capacity of the cellular steel beam, the vertical stiffeners can be installed.

The beam analysed at the web post buckling due to the compression force failure mode is presented in Figure 30. This beam is simply supported, and its upper flange is restrained out of plain at the force application places. This beam is loaded with the concentrated forces. The beam parameters are: b_f=160 mm, t_f=16 mm, h_w=1000 mm, t_w=6 mm, d=700 mm, a=150 mm, L=9000 mm, F=100.6 kN, f=40 mm, M=640.6 kg, R=0.314 kN/kg.

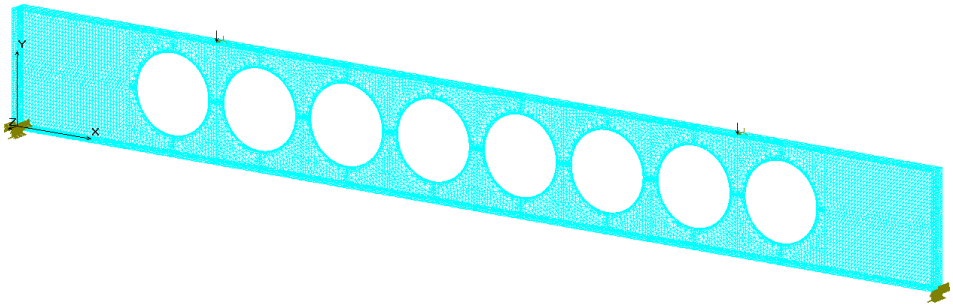

Figure 30. The supporting and loading model of the beam analysed at the web post buckling due to the compression force failure mode

The deformed shape of the beam at the web post buckling due to the compression force failure mode is presented in Figure 31. From this picture it is seen, that the value of the horizontal deflection is bigger than that of the vertical one, and it almost reached the ultimate value. Under the load application point the web post buckles out of plain. At the same time the flanges twist what causes the buckling of the nearest web posts.

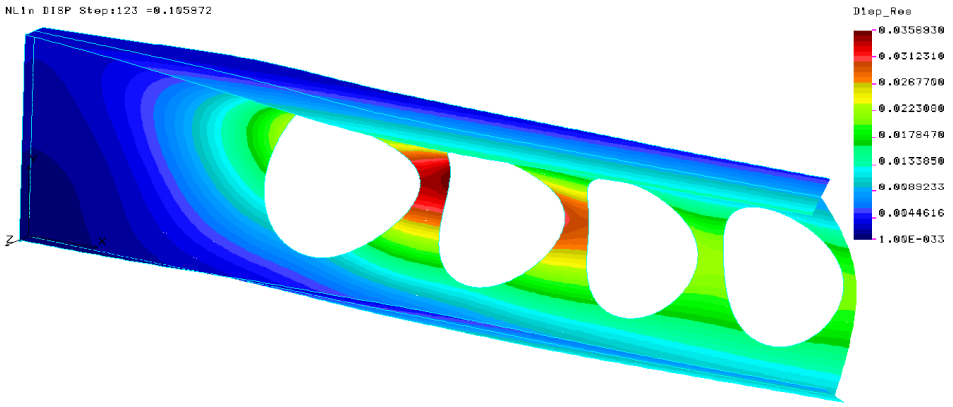

Figure 31. Deformed shape of the beam at the web post buckling due to the compression force failure mode

From the Figures 31–35 it is seen that the main stress component which caused the web post buckling is τ_{xy}.

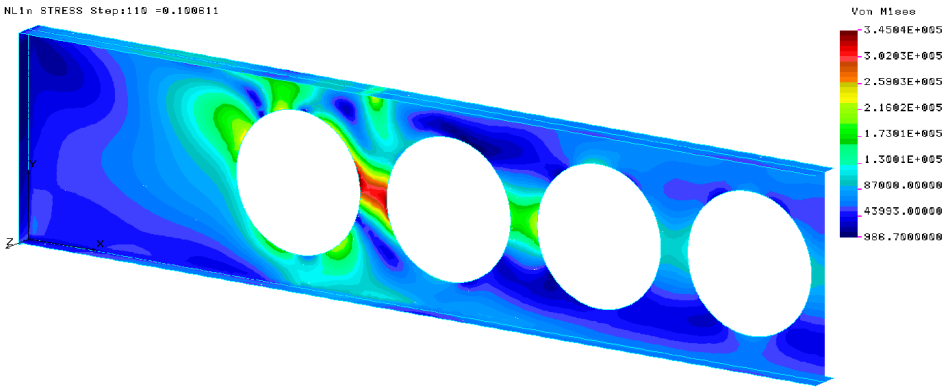

Figure 32. Distribution of the Von Mises stresses along the beam at the web post buckling due to compression force failure mode

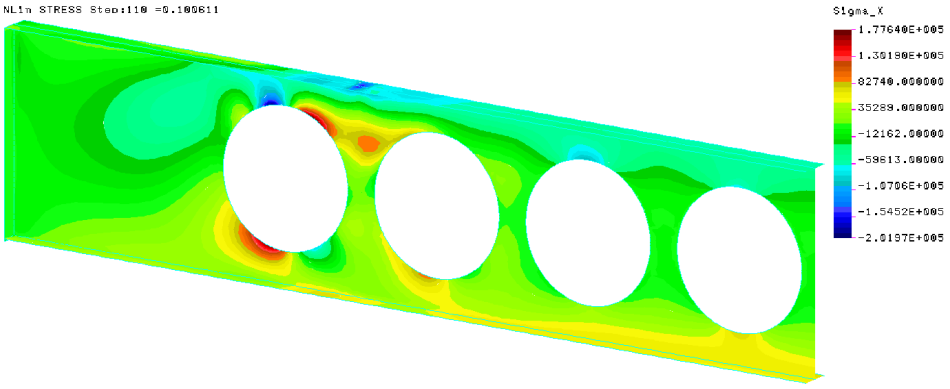

Figure 33. Distribution of the stresses σ_x along the beam at web post buckling due to compression force failure mode

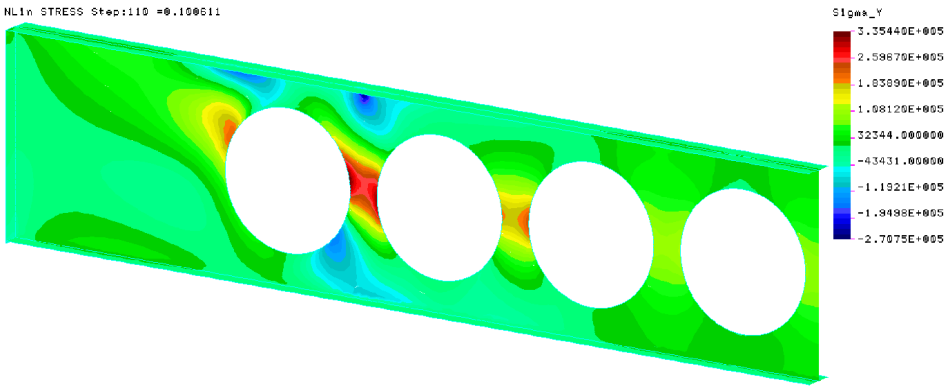

Figure 34. Distribution of the stresses σ_y along the beam at web post buckling due to compression force failure mode

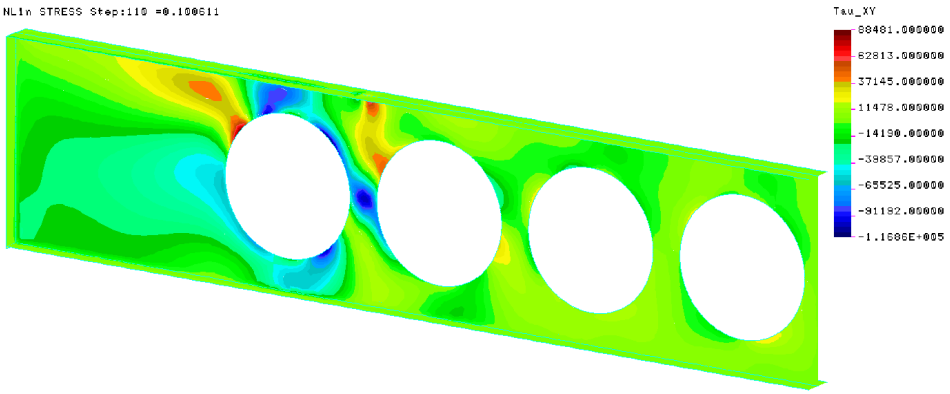

Figure 35. Distribution of the stresses τ_{xy} along the beam at web post buckling due to compression force failure mode

4.6 Failure mode – Vierendeel or shear mechanism

This mode of failure usually occurs in beams, which are short and T-sections above and below the openings are sufficiently small. Then the share force acts the beam, T-sections above and below the openings have to carry the share force and primary and secondary bending moments. The primary bending moment is usual bending moment which acts the beam. The secondary bending moment, also called Vierendeel moment, arise from a share forces in T-sections.

The beam analysed at the Vierendeel or shear mechanism failure mode is presented in Figure 36. This beam is simply supported, and its upper flange along the all length is restrained out of plain. Beam is loaded with uniformly distributed load. The beam parameters are: b_f=140 mm, t_f=14 mm, h_w=1000 mm, t_w=12 mm, d=700 mm, a=150 mm, L=8000 mm, p=70.1 kN/m, f=35 mm, M=559.0 kg, R=1.000 kN/kg.

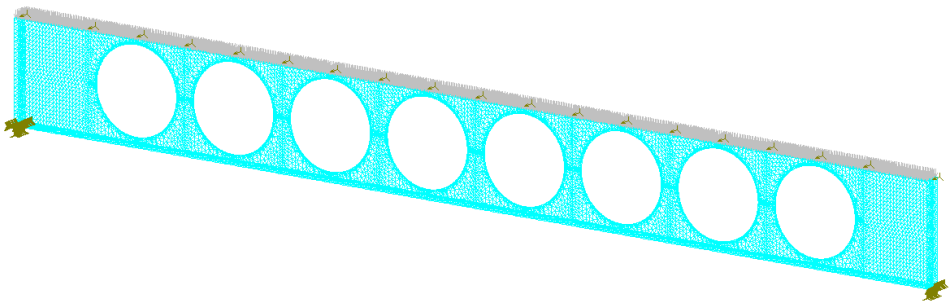

Figure 36. The supporting and loading model of the beam analysed at the Vierendeel or shear mechanism failure mode

In Figure 37 it is seen the shift in the T-sections below and above the opening. The closer opening is to the end of the beam, the bigger shift of T-sections is below and above the opening. No lateral deformation is observed.

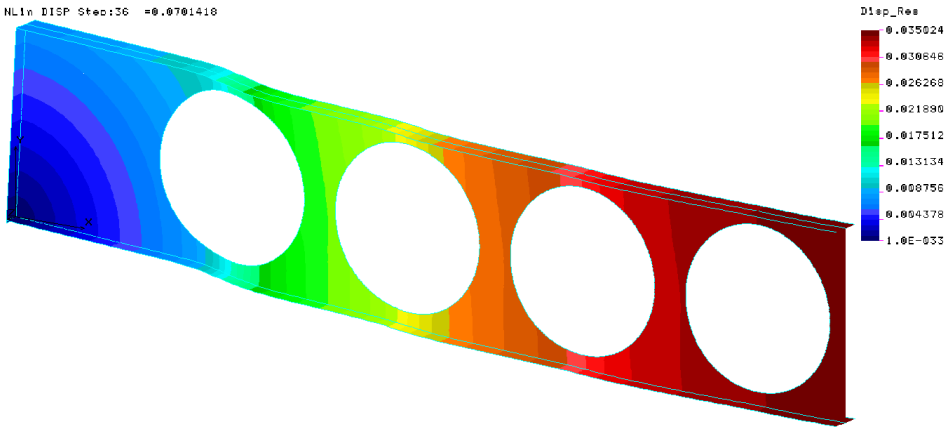

Figure 37. Deformed shape of the beam at the Vierendeel or shear mechanism failure mode

From the Figures 38–41 it is seen that the main stress components which caused the web post buckling are σ_x and τ_{xy}. The flanges and the web of T-sections below and above the opening reached the yielding stresses. It can be noted that the secondary bending moment has more influence on formation of Vierendeel mechanism than the primary bending moment, because the further openings are from the end of the beam, the smaller stresses are observed.

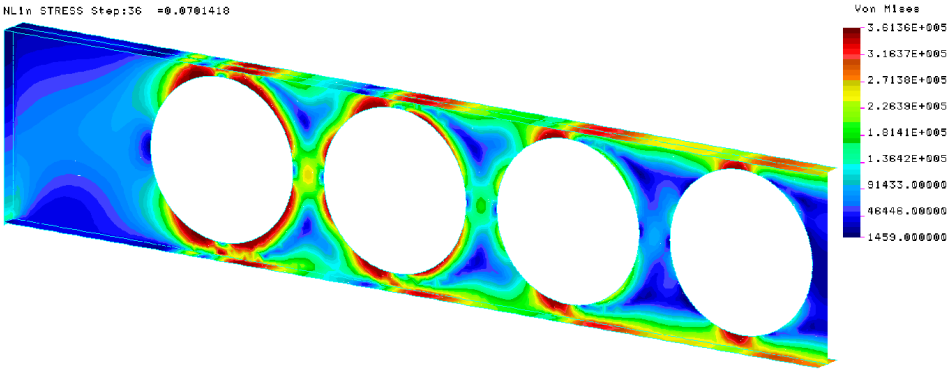

Figure 38. Distribution of the Von Mises stresses along the beam at the Vierendeel or shear mechanism failure mode

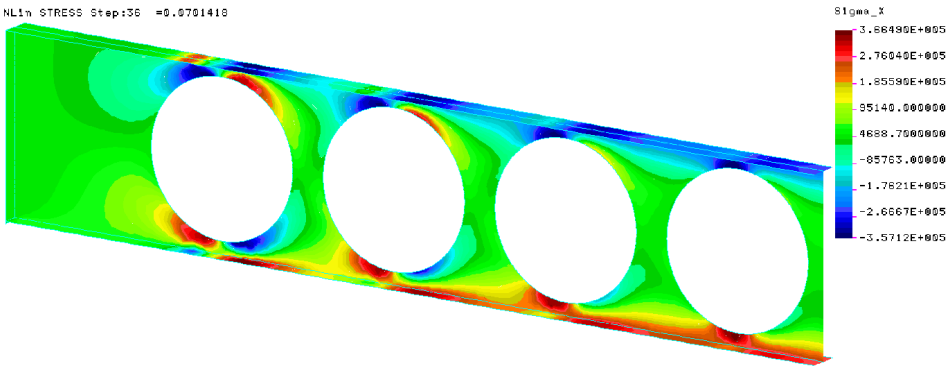

Figure 39. Distribution of the stresses σ_x along the beam at Vierendeel or shear mechanism failure mode

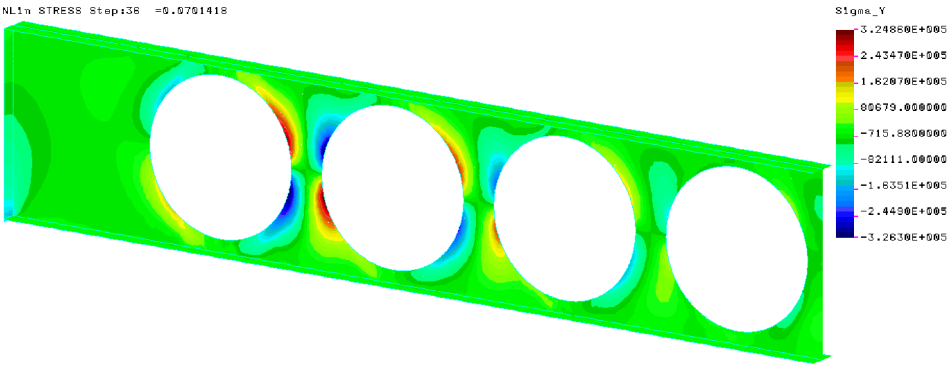

Figure 40. Distribution of the stresses σ_y along the beam at Vierendeel or shear mechanism failure mode

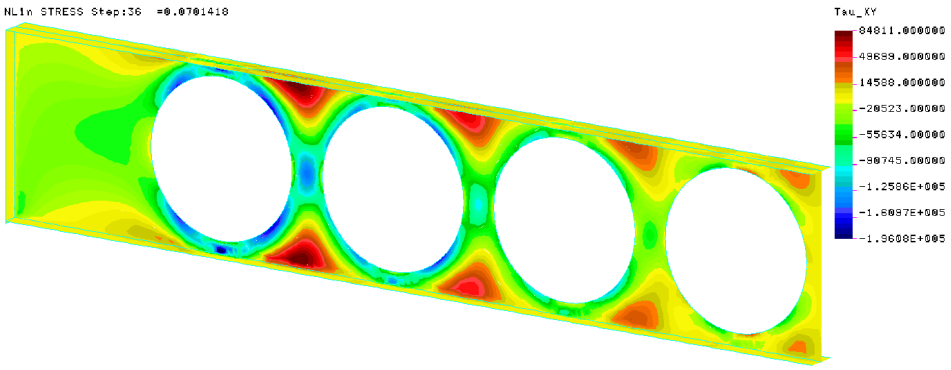

Figure 41. Distribution of the stresses τ_{xy} along the beam at Vierendeel or shear mechanism failure mode

5 Some ideas how to develop a method for selection of rational cross-sectional dimensions of cellular steel beams

There are a few principles how to obtain the rational cross-sectional dimensions. One of them requires difficult mathematical calculations, because there are many conditions which are limiting the depth of the beam and the diameter of the openings, the distance between the openings, and etc. Other method requires preparing some database from which the needed beam with rational cross-sectional dimensions can be easily selected. This concept is very simple. First of all it is necessary to make some assumptions: the beam is simply supported, its upper flange is restrained out of plain; the acting load is uniformly distributed; the length of the beam is L=6000 mm; the web depth is h_w=350–500 mm, every 50 mm; the web thickness is t_w=5–6 mm, every 1 mm; the flange thickness t_f is equal to double thickness of the web; the flange width is $b_f=h_w/4$; the diameter of the opening is d=200–400 mm, every 50 mm; the distance between the openings is a=150 mm; the ultimate deflection f=30 mm; a number of the openings is chosen so, that the distance from the end of the beam to the edge of the first opening would be minimal, but not less than 250 mm; the minimum distance from the edge of the opening to the flange is 50 mm. After this, the charts R=f(d) like presented in Figure 42 for any web thickness and web depth are being created.

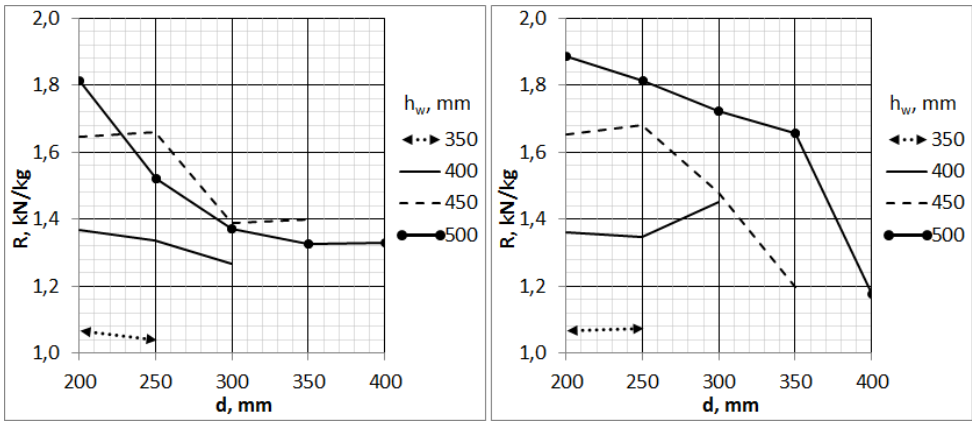

a) b)

Figure 42. Relationship of R versus d, a) for t_w=5 mm, b) for t_w=6 mm

Using such charts, the beams with maximum value of R can be selected as the beam of the rational cross-sectional dimensions.

5.1 Example of selection the rational cross-sectional dimension of cellular beam

Let to assume that there are 30 beams in the database (the number of the beams can be any), which is presented in Figure 42. There are two ways how to select the rational dimensions of the cellular steel beam.

First method:

1. There are some conditions limiting web depth and openings diameter;
2. According to the conditions mentioned above the beam with maximum R value can be selected. In our case it is the beam with h_w=500 mm, t_w=6 mm, b_f=125 mm, t_f=12 mm, d=200 mm, M=258.92 kg, R=1.888 kN/kg, p=81.47 kN/m;
3. There is some load acting on beam per m^2. For example if it is car parking, the total design load can be g=11.0 kN/m^2;
4. Spacing between the beams b can be easily found using formula b=p/g=81.47/11=7.4 m.

Second method (this method may be used when spacing between beams is too big):

1. There are some conditions limiting openings diameter, beams spacing b=6.0 m and load g=11.0 kN/m^2 are given. So p load can be easily calculated and it is p=b·g=6.0·11=66 kN/m;
2. Using formula R=p·L/M, where M is function of h_w and steel density is taken 7850 kg/m^3, h_w can be easily expressed as it shown in Equation (1).

$$h_w = \frac{p}{15700 \cdot R \cdot t_w} + \frac{0.3982 \cdot N \cdot d^2}{L} \qquad (1)$$

3. From the charts presented in Figure 42 the beams with highest R values are being selected. For example just select three beams:
   a) R=1.888 kN/kg, t_w=6 mm, h_w=500 mm, d=200 mm, N=16;
   b) R=1.815 kN/kg, t_w=6 mm, h_w=500 mm, d=250 mm, N=14;
   c) R=1.812 kN/kg, t_w=5 mm, h_w=500 mm, d=200 mm, N=16;
4. For all selected beams according to the Equation (1) h_w are being calculated. In our case for (a) beam h_w=413 mm, (b) beam h_w=443 mm, (c) beam h_w=506 mm;
5. From selected beams, the beam with h_w value, calculated according to the Equation (1), which is closest to h_w value of selected beams is selecting. In our case the beam with the rational cross-sectional dimensions is the beam (c).

6 Conclusions

Six modes of failure were presented and overviewed in this paper. The finite element analysis of cellular steel beams performed showed that:

- Material of the beam is used efficiently when the beam fails according to the flexural mechanism mode;
- The stresses around the beam end openings has a local character and they do not distribute widely, except the case when T-sections below and above the opening are small enough.
- The main failure mode, when beam is longer than six–seven meters is exceeding the ultimate deflection.

Moreover, the principles of selecting the rational dimensions of cellular beams was presented in this paper. Of course, this principle should be considered together with the design code requirements. In the future work a possibility exists for selecting the rational cross-sectional dimensions of cellular steel beams to develop else more simple method.

References

[1] A. Čižas, “Mechanics of materials. Mechanics of structural elements”, Technika, Vilnius, 1993.

[2] N. E. Shanmugam, V. T. Lian and V. Thevendran, “Finite element modelling of plate girders with web openings”, Thin-Walled Structures 40(5), 443-464, 2002.

[3] J. D. Megharief, “Behaviour of composite castellated beams”, MSc Thesis, McGill University, Montreal, 1997.

[4] A. Mohebkhah, “The moment-gradient factor in lateral-torsional buckling on inelastic castellated beams”, Journal of Constructional Steel Research 60(10), 1481-1494, 2004.

[5] T. Zirakian, H. Showkati, “Distortional buckling of castellated beams”, Journal of Constructional Steel Research 62(9), 863-871, 2006.

[6] D. Kerdal, D. A. Nethercot, “Failure modes for castellated beams”, Journal of Constructional Steel Research 4(4), 295-315, 1984.